Journal of Science and Technology in Civil Engineering, HUCE, 2023, 17 (4): 26–36

TRANSIENT ANALYSIS OF FUNCTIONALLY GRADED PLATES USING EXTREME GRADIENT BOOSTING

Dieu T. T. Do[a,*], Son Thai[b,c]

[a]*Faculty of Information Technology, Nguyen Tat Thanh University, 331, 1A Street An Phu Dong Ward, District 12, Ho Chi Minh city, Vietnam*
[b]*Faculty of Civil Engineering, Ho Chi Minh City University of Technology (HCMUT), 268 Ly Thuong Kiet street, Ward 14, District 10, Ho Chi Minh city, Vietnam*
[c]*Vietnam National University Ho Chi Minh City (VNU-HCM), Linh Trung ward, Thu Duc city, Ho Chi Minh city, Vietnam*

Article history:
Received 23/8/2023, Revised 27/9/2023, Accepted 10/10/2023

Abstract

This paper is aimed at quickly predicting the dynamic behavior of functionally graded plates using non-traditional computational approaches consisting of artificial neural networks (ANN) and extreme gradient boosting (XGBoost). Through the use of ANN and XGBoost, the dynamic behavior of the plate can be directly predicted based on optimal mapping, which is found by learning the relationship between input and output data from a data set during the training process. A data set including 1000 data pairs (input and output) is generated by using a combination of isogeometric analysis (IGA) and third-order shear deformation plate theory through iterations. In this model, a power index that controls the plate's material distribution is regarded as input, and output consists of 200 values of deflection versus time. In order to demonstrate the effectiveness of XGBoost in terms of accuracy and computational time, results obtained by the optimal XGBoost model are compared to those obtained by the optimal ANN model and IGA.

Keywords: functionally graded plate; isogeometric analysis (IGA); transient analysis; artificial neural network (ANN); extreme gradient boosting (XGBoost).

https://doi.org/10.31814/stce.huce2023-17(4)-03

1. Introduction

Functionally graded materials (FGMs), a type of smart materials, are typically composed of two constituents: ceramic and metal. The material properties change in directions. The outstanding properties of FGMs are derived from the ceramic's ability to withstand high temperatures and the metal's remarkable fracture toughness. FGMs have the ability to completely eliminate undesired stress discontinuity in laminated composite layers. Therefore, FGMs are increasingly being used in a variety of fields such as nuclear power plants [1], aircraft engineering [2], biological [2], and so on.

Dynamic analysis problems for functionally graded plates are currently attracting many researchers around the world due to their outstanding features and practical applications in a variety of fields. For instance, Raveen and Reddy [3] investigated the static and dynamic responses of functionally graded plates using a simple power law distribution to vary the volume fraction of metal and ceramic. Ootao et al. [4] investigated the transient thermoelastic problem of a functionally graded plate with piecewise exponential law caused by a nonuniform heat supply. Tran and Thai [5] used isogeometric analysis to investigate transient analysis of multi-directional functionally graded plates. And several other studies as shown in [6, 7]. In the aforementioned studies, most of the studies have used traditional analytical methods. This would be time-consuming and computationally expensive. Therefore, in this study,

*Corresponding author. *E-mail address:* dttdieu@ntt.edu.vn (Do, D. T. T.)

an effective machine learning (ML) method named extreme gradient boosting (XGBoost) has been proposed for the dynamic analysis of functionally graded plates to reduce computational time while ensuring accuracy.

XGBoost [8], developed by Chen and Guestin in 2016, is a combination of several gradient-boosted decision trees that have been specifically designed for high predictive accuracy and computational efficiency. This is one of the most well-known ML algorithms, having won numerous competitions between ML algorithms organized by Kaggle, the world's most popular forum for data scientists. XGBoost is frequently used to solve supervised learning problems with high accuracy and has been used successfully in a variety of fields [9–14]. For instance, Zhang et al. [9] constructed four models to analyze the mechanisms of radon variation under natural and seismic conditions using XGBoost. Zou et al. [10] developed XGBoost model to assess central cervical lymph node metastasis, consisting of positive and negative effects. However, no research has been carried out to investigate the effectiveness of XGBoost in predicting the dynamic behavior of functionally graded plates.

In order to create a dataset for the training process in the XGBoost, isogeometric analysis [15] (IGA) has been proposed for this data generation process to ensure the accuracy of the solution. IGA was proposed as a method of combining CAD and FEA. IGA employs the same non-uniform rational B-spline (NURBS) to represent both exact CAD geometry and approximate FEA solution fields. Furthermore, the exact geometry is preserved even at the coarsest discretization level, and this method is effective in reducing degrees of freedom (DOFs) for high-order elements. As a result, IGA has been applied in a wide range of engineering fields [16–18]. For instance, Son and Qui [16] investigated the static bending and free vibration behavior of multi-directional functionally graded plates with variable thickness. The accuracy of the proposed method has been demonstrated through numerical examples. Farahat et al. [17] presented an isogeometric method for analyzing complex Kirchhoff-Love shells in which the shell's mid-surface is approximated by a particular class of G1-smooth multi-patch surfaces known as AS-G1. The numerical results demonstrated the proposed method's great potential for efficient shell analysis of geometrically complex multi-patch structures that cannot be modeled without the use of extraordinary vertices.

In this study, the dynamic behavior of the FG plate is first examined using a combination of isogeometric analysis (IGA) and third-order shear deformation plate theory (TSDT). The accuracy of the method is validated by comparing the obtained results to those in the literature. The above combination then generates a data set consisting of 1000 data pairs, each of which includes a power index that controls the plate's material distribution as input, and output consisting of 200 values of deflection versus time through iterations. This data set is used in the training process of ML methods such as artificial neural networks (ANN) and XGBoost to determine optimal weights. Based on these weights, outputs will be predicted directly from the input without the use of any analysis tools. Furthermore, the effect of parameters on the accuracy and computational time of ANN and XGBoost will be investigated in order to find optimal models. The results of these optimal models and IGA are compared to validate the effectiveness and robustness of XGBoost.

2. Isogeometric analysis of functionally graded plates

2.1. Plate formulation

In this study, third-order shear deformation plate theory (TSDT) proposed by Reddy [19] is used to describe the displacement field of any point in the plate, as given below:

$$\left\{\begin{array}{c} u_1 \\ u_2 \\ u_3 \end{array}\right\} = \left\{\begin{array}{c} u \\ v \\ w \end{array}\right\} + f(z)\left\{\begin{array}{c} \theta_x \\ \theta_y \\ 0 \end{array}\right\} - g(z)\left\{\begin{array}{c} \dfrac{\partial w}{\partial x} \\ \dfrac{\partial w}{\partial y} \\ 0 \end{array}\right\} \tag{1}$$

where $u, v,$ and w denote the spatial translations; θ_x and θ_y represent the angular deformations; $f(z)$ and $g(z)$ are described as follows

$$f(z) = z - \frac{4z^3}{3h^2}; \quad g(z) = \frac{4z^3}{3h^2} \tag{2}$$

in which z represents the coordinate in the direction of thickness, while h denotes the thickness of the plates.

According to the infinitesimal elasticity theory, the strain-displacement relations are described as follows:

$$\varepsilon_{xx} = \frac{\partial u}{\partial x} + f(z)\frac{\partial \theta_x}{\partial x} - g(z)\frac{\partial^2 w}{\partial x^2} \tag{3}$$

$$\varepsilon_{yy} = \frac{\partial v}{\partial y} + f(z)\frac{\partial \theta_y}{\partial y} - g(z)\frac{\partial^2 w}{\partial y^2} \tag{4}$$

$$\gamma_{xy} = \frac{\partial u}{\partial y} + \frac{\partial v}{\partial x} + f(z)\left(\frac{\partial \theta_x}{\partial y} + \frac{\partial \theta_y}{\partial x}\right) - g(z)\left(\frac{\partial^2 w}{\partial x \partial y} + \frac{\partial^2 w}{\partial x \partial y}\right) \tag{5}$$

$$\gamma_{xz} = f'(z)\theta_x + (1 - g'(z))\frac{\partial w}{\partial x} \tag{6}$$

$$\gamma_{yz} = f'(z)\theta_y + (1 - g'(z))\frac{\partial w}{\partial y} \tag{7}$$

The linear elastic constitutive equation for the plate issue is provided by

$$\sigma_{xx} = Q_{11}\varepsilon_{xx} + Q_{12}\varepsilon_{yy} \tag{8}$$

$$\sigma_{yy} = Q_{21}\varepsilon_{xx} + Q_{22}\varepsilon_{yy} \tag{9}$$

$$\sigma_{xy} = Q_{44}\gamma_{xy}; \quad \sigma_{yz} = Q_{55}\gamma_{xy}; \quad \sigma_{xz} = Q_{66}\gamma_{xy} \tag{10}$$

in which

$$Q_{11} = Q_{22} = \frac{E}{1-\nu^2}; \quad Q_{12} = Q_{21} = \frac{E\nu}{1-\nu^2}; \quad Q_{44} = Q_{55} = Q_{66} = \frac{E}{2(1+\nu)} \tag{11}$$

where $E = E(z)$ and $\nu = \nu(z)$ are the Young's modulus and Poisson's ratio, respectively. In this study, it is assumed that these quantities and the mass density (ρ) vary throughout the thickness of the plate and are defined as follows:

$$E(z) = E_c V_c + E_m V_m \tag{12}$$

$$\nu(z) = \nu_c V_c + \nu_m V_m \tag{13}$$

$$\rho(z) = \rho_c V_c + \rho_m V_m \tag{14}$$

in which c and m represent ceramic and metal constituents, respectively; $V_c(z)$ and $V_m(z)$ are the volume fractions of ceramic and metal, respectively; and $V_c + V_m = 1$.

By employing Hamilton's principle, the equation of motion for the given problem can be expressed as follows:

$$\int_{-h/2}^{h/2} (\delta T - \delta U - \delta W_e)\, dt = 0 \tag{15}$$

where T denotes the kinetic energy, U represents the elastic energy, and W_e denotes the work done by external forces. The formulations for the variational form of these terms are provided by

$$\delta T = \int_V \rho \ddot{u}_i \delta u_i dV \tag{16}$$

$$\delta U = \int_V \sigma_{ij} \delta \varepsilon_{ij} dV \tag{17}$$

$$\delta W_e = -\int_\Gamma \hat{t}_i \delta u_i d\Gamma \tag{18}$$

in which V is the volume of the plate; $\hat{t}_i$ denotes the external loads acting on the area Γ; and the dot superscript represents the derivative with respect to time t.

The equation of motion can be rewritten as follows by replacing Eq. (15) with Eqs. (3)–(7) and (16)–(18), and making some arrangements:

$$\int_\Omega \delta \hat{\boldsymbol{\varepsilon}}^T \hat{\mathbf{D}} \hat{\boldsymbol{\varepsilon}} d\Omega + \int_\Omega \delta \bar{\mathbf{u}}^T \mathbf{m} \ddot{\bar{\mathbf{u}}} d\Omega = \int_\Omega q(t)\, \delta w d\Omega \tag{19}$$

where Ω represents the reference plane of the plate; $q(t)$ is the distributed load exerted on the upper surface of the plate and is dependent on the variable of time t. Readers can consult Ref. [5] for specific information about the quantities mentioned in the equation above.

2.2. *Isogeometric analysis*

In this study, the IGA method [15] is employed to model the plate. The equation of motion is discretized using the NURBS basis function $R_{i,j}^{p,q}(\xi, \eta)$. The displacement $\mathbf{u}$ of the eth NURBS element is given by

$$\mathbf{u} = \sum_{i=1}^{ncp} R_i(\xi, \eta)\, \mathbf{d}_i \tag{20}$$

where $\mathbf{u} = \left\{ \begin{array}{ccccc} u & v & \theta_x & \theta_y & w \end{array} \right\}^T$ symbolizes the displacement vector, $\mathbf{d}_i = \left\{ \begin{array}{ccccc} u_i & v_i & \theta_{xi} & \theta_{yi} & w_i \end{array} \right\}^T$ denotes the corresponding variables for displacement associated with the ith control point.

By substituting Eq. (20) into Eq. (19), the equation for the system is reformulated as follows:

$$\mathbf{M}\ddot{\mathbf{d}} + \mathbf{K}\mathbf{d} = \mathbf{q}(t) \tag{21}$$

where $\mathbf{M}$ and $\mathbf{K}$ are the mass and stiffness matrices, respectively; and $\mathbf{q}(t)$ symbolizes the load vector. More information on these quantities can be found in [5].

Only structural damping of the plate is taken into account in this study. The damping is modeled using the Rayleigh damping method, with the proportional damping matrix defined by

$$\mathbf{C} = a_0 \mathbf{M} + a_1 \mathbf{K} \tag{22}$$

where

$$a_1 = \frac{2\zeta}{\omega_1 + \omega_2}; \quad a_0 = \omega_1 \omega_2 a_1 \tag{23}$$

in which ζ is the damping ratio of the first and the second vibration modes; ω_1 and ω_2 are the natural frequencies of the first and the second vibration modes, respectively.

The equation of the system in Eq. (21) incorporating the damping matrix is rewritten as follows:

$$\mathbf{M}\ddot{\mathbf{d}} + \mathbf{C}\dot{\mathbf{d}} + \mathbf{K}\mathbf{d} = \mathbf{q}(t) \tag{24}$$

To address the time-dependent issue as explained in Eq. (24), the Newmark technique [20] is utilized. Readers can refer to Ref. [5] for the general procedure for solving the transient problem.

3. Extreme gradient boosting (XGBoost)

XGBoost is an implementation of gradient boosting machines, which is known as one of the best-performing supervised learning algorithms. It can be employed for regression as well as classification problems. XGBoost has received a lot of attention from researchers, especially data scientists, because of its fast execution speed and core computing capabilities. The implementation of an XGBoost model begins with a dataset of n observations with independent variables x_i, each of which has m unique features, and thus $x_i \in \mathbb{R}^m$. There is a dependent variable (desired value) y_i that corresponds to each row of x_i variables, as $y_i \in \mathbb{R}$. XGBoost model will predict $\hat{y}_i$ based on the independent variables (input values) as follows:

$$\hat{y}_i = \sum_{k=1}^{K} f_k(x_i), \; f_k \in F \tag{25}$$

where K symbolizes the number of trees in the model; f_k denotes the kth tree; and F symbolizes the space of regression trees.

To solve the aforementioned equation, the best set of functions needs to be found by minimizing the loss and regularization objective as follows:

$$L(\varphi) = \sum_i l(\hat{y}_i, y_i) + \sum_k \Omega(f_k) \tag{26}$$

in which l stands for the loss function, which is the difference between the predicted output $\hat{y}_i$ and the actual output y_i; and Ω is a measure of the model's complexity, which helps prevent over-fitting of the model and is derived by:

$$\Omega(f_k) = \gamma T + \frac{1}{2}\lambda \|w_i\|^2 \tag{27}$$

where T and w_i are the number of leaves and the scores or weights of ith leaf, respectively.

From Eqs. (25)–(27), the optimal weights w_j^* and the corresponding values can be gained as follows:

$$w_j^* = -\frac{\sum_{i \in I_j} \partial_{\hat{y}^{t-1}} l\left(y_i, \hat{y}^{t-1}\right)}{\sum_{i \in I_j} \partial^2_{\hat{y}^{t-1}} l(y_i, \hat{y}^{t-1}) + \lambda} \tag{28}$$

$$L^t = -\frac{1}{2}\sum_{j=1}^{T} \frac{\left(\sum_{i \in I_j} \partial_{\hat{y}^{t-1}} l\left(y_i, \hat{y}^{t-1}\right)\right)^2}{\sum_{i \in I_j} \partial^2_{\hat{y}^{t-1}} l(y_i, \hat{y}^{t-1}) + \lambda} + \gamma T \tag{29}$$

Because it is complicated to solve the aforementioned equations for all possible tree structures, the exact greedy algorithm [8] is frequently used to produce a more generalized and simplified formula, which is described as follows:

$$L_{split} = \frac{1}{2}\left[\frac{\left(\sum\limits_{i\in I_L}\partial_{\hat{y}^{t-1}} l\left(y_i,\hat{y}^{t-1}\right)\right)^2}{\sum\limits_{i\in I_L}\partial^2_{\hat{y}^{t-1}} l\left(y_i,\hat{y}^{t-1}\right)+\lambda} + \frac{\left(\sum\limits_{i\in I_R}\partial_{\hat{y}^{t-1}} l\left(y_i,\hat{y}^{t-1}\right)\right)^2}{\sum\limits_{i\in I_R}\partial^2_{\hat{y}^{t-1}} l\left(y_i,\hat{y}^{t-1}\right)+\lambda} - \frac{\left(\sum\limits_{i\in I}\partial_{\hat{y}^{t-1}} l\left(y_i,\hat{y}^{t-1}\right)\right)^2}{\sum\limits_{i\in I}\partial^2_{\hat{y}^{t-1}} l\left(y_i,\hat{y}^{t-1}\right)+\lambda}\right] - \gamma \tag{30}$$

in which $I = I_L \cup I_R$; I_L and I_R symbolize the instances sets of left and right nodes after the split, respectively.

4. Numerical examples

In this study, the dynamic behavior of isotropic square plate is investigated to verify the accuracy of the combination of IGA and TSDT. Following that, XGBoost and ANN are used in place of IGA to quickly analyze the behavior of the FG plate. In which the plate is composed of Al_2O_3/Al components with material properties as follows:

Ceramic Al_2O_3: $E_c = 380$ GPa, $v_c = 0.3, \rho_c = 3800$ kg/m^3
Metal Al: $E_m = 70$ GPa, $v_m = 0.3, \rho_m = 2707$ kg/m^3

The material distribution varies in the direction of the Al_2O_3/Al plate's thickness as follows:

$$V_c = \left(\frac{z}{h} + \frac{1}{2}\right)^{n_z} \tag{31}$$

in which V_c denotes the ceramic volume fraction; h is the thickness of the plate; n_z represents the power index in the z-axis.

A data set consiting of 1000 data pairs in XGBoost and ANN is generated by the combination of IGA and TSDT. In which n_z is considered as input with value changes from 0 to 10; output comprises 200 values of deflection versus time which is described as follows:

$$\bar{t} = t\sqrt{\frac{E_m}{a^2\rho_m}}; \quad \bar{w} = \frac{10^3 D_0}{q_0 a^4} w; \quad D_0 = \frac{E_c h_0^3}{12\left(1-v_c^2\right)} \tag{32}$$

This data set is divided into two small groups: 900 data pairs used for the training process; and the remaining 100 data pairs used for the testing process in XGBoost and ANN. To select an optimal model for ANN, the influence of the optimizer, activation function, epoch, and the number of hidden layers and nodes on ANN effectiveness is examined. Besides, the effect of the number of trees (n_estimators), maximum depth of a tree (max_depth) and learning rate (eta) on the effectiveness of XGBoost is investigated to choose an optimal model of XGBoost. The optimal models for ANN and XGBoost are then contrasted with one another in terms of accuracy and computational efficiency.

The process of the training is performed by Python 3.7 and carried out via programs on laptop with Intel®Core^{TM} i7-8550U CPU @ 1.80 GHz 2.00 GHz, 12.0 GB RAM of memory, and Windows 11 with 64-bit operating system.

4.1. Verification

The dynamic problem of a square isotropic plate that Kant et al. [21] and Lei et al. [22] addressed is first reviewed to verify the accuracy of the present method. The thickness and side length of the plate are $h = 0.05$ m and $a = 0.25$ m, respectively. The material properties of this plate are Young's modulus $E = 2.1 \times 10^{10}$ N/m^2, Poisson's ratio $\nu = 0.25$, and density $\rho = 800$ kg/m^3. This plate is subjected to a sudden uniformly distributed dynamic load with $q = 0.1 \times 10^5$ N/m^2 under simply supported (SSSS) boundary condition which is given as follows:

$$\begin{aligned} u = \theta_x = w = 0 \text{ at } y = 0, y = b \\ v = \theta_y = w = 0 \text{ at } x = 0, x = a \end{aligned} \tag{33}$$

A comparison of results gained by the present method and those of referenced studies is presented in Fig. 1. From the figure, it can be seen that the present results agree well with those of previous studies.

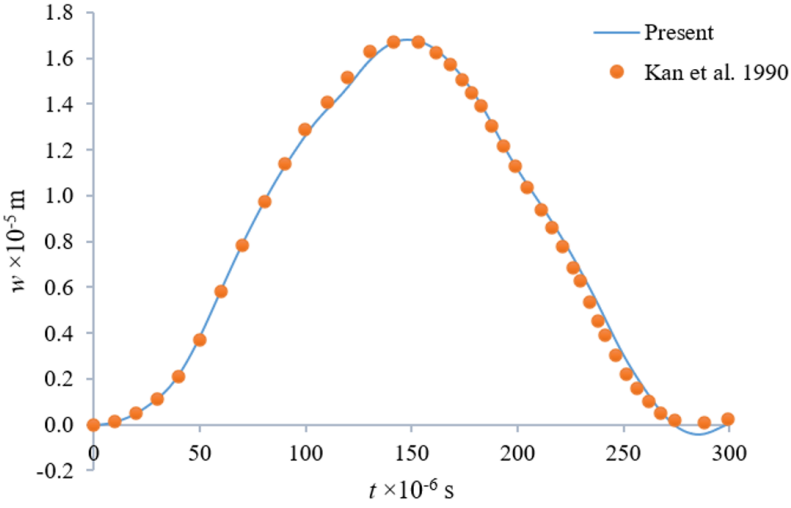

Figure 1. Comparison of centre deflection versus time of square isotropic plates with previous studies

4.2. Applying ANN and XGBoost for predicting dynamic behaviors of the FG plate

In this section, dynamic behavior of the Al_2O_3/Al square plate with $h = a/20$ is examined. The plate is subjected to a sudden uniformly distributed dynamic load with $q_0 = -0.5 \times 10^8$ N/m^2 under CCCC boundary condition that is shown as follows:

$$u = v = \theta_x = \theta_y = w = \frac{\partial w}{\partial n} = 0 \text{ at all edges} \tag{34}$$

In this example, the damping ratio ζ of 0.05 is taken into account. The data set including 1000 data pairs is generated by the combination of IGA and TSDT through iterations.

The application of ANN for predicting the FG plate's deflection center versus time is first investigated. An ANN architecture which consists of two hidden layers with 50 neurons each hidden layer, 1 input, and 200 outputs is considered in the first investigation to find an optimal combination of optimizer and activation function. In particular, 5 optimizers are examined, including Adam, RMSprop, Adagrad, SGD, and Adadelta, as well as 6 activation functions, including linear, sigmoid, softmax, softplus, tanh, and ReLU. The results are shown in Table 1. Mean square error (MSE), mean

absolute percentage error (MAPE), and computational time for training and testing processes after 1000 epochs are used to evaluate the effectiveness of various combinations of optimizers and activation functions. According to the table, the combination of Adam optimizer and ReLU function gives the lowest MSE (1.37E-5 for training and 3.60E-5 for testing) and MAPE (0.4550% for training and 0.9773% for testing). This combination takes around 16 seconds to train and test. Fig. 2 depicts the convergence history of the Adam and ReLU combination. The graph indicates that the loss (MSE) of both the training and testing processes converges to zero. As a result, this combination is used in subsequent investigations.

Table 1. Comparison of the effect of various optimizer and activation function combinations on the accuracy of the training and testing processes in ANN

			Optimizer									
			Adam		RMSprop		Adagrad		SGD		Adadelta	
			Training	Testing	Training	Testing	Training	Testing	Training	Testing	Training	Testing
Activation function	Linear	MSE	0.0005	0.0009	0.0005	0.0008	0.0006	0.0015	0.0036	0.0063	0.0005	0.0011
		MAPE	3.1521	5.5602	3.1506	4.9649	3.1994	7.3267	8.5631	15.6713	3.0856	6.2279
		Time (second)	13.2803		12.4348		13.9109		14.7382		18.6366	
	Sigmoid	MSE	0.0001	0.0002	0.0003	0.0003	0.0005	0.0008	0.0018	0.0019	0.0016	0.0015
		MAPE	1.1934	2.1061	2.3094	2.8185	3.0490	5.0270	5.8368	8.2550	5.5188	7.2935
		Time (second)	19.2116		19.2316		19.4978		18.2508		19.8407	
	Softmax	MSE	0.0001	0.0001	0.0001	0.0002	0.0009	0.0003	0.0261	0.0151	0.0018	0.0019
		MAPE	1.0261	1.9580	1.2263	2.7306	3.6372	2.9887	28.9558	23.8606	5.8382	8.2601
		Time (second)	19.5292		19.1123		18.2047		19.0603		20.6348	
	Softplus	MSE	0.0001	0.0005	0.0006	0.0003	0.0005	0.0009	0.0019	0.0021	0.0005	0.0011
		MAPE	1.5143	3.7556	3.6047	3.2394	3.0296	5.5363	5.9485	8.5972	3.0304	6.0401
		Time (second)	32.8799		27.9835		30.6368		28.2664		29.1650	
	Tanh	MSE	0.0001	0.0001	0.0001	0.0003	0.0004	0.0006	0.0030	0.0046	0.0005	0.0011
		MAPE	0.9636	1.3040	1.7097	1.7097	2.5858	4.2623	7.7766	13.2956	3.0751	6.2054
		Time (second)	15.9581		13.7303		14.3317		12.5754		14.4344	
	ReLU	MSE	1.37E-05	3.60E-05	4.17E-05	5.99E-05	1.04E-04	1.52E-04	3.63E-03	6.21E-03	4.68E-04	8.02E-04
		MAPE	0.4550	0.9773	1.0948	1.3951	1.1507	2.0508	8.6151	8.6151	2.9421	5.1056
		Time (second)	16.1840		13.4401		12.9469		11.7047		14.0394	

The impact of the number of epochs in ANN with Adam optimizer and ReLU function is then examined. The obtained results are tabulated in Table 2. As shown in the table, the ANN with 3000 epochs gives the best results. Thus, ANN with Adam optimizer, ReLU function, and 3000 epochs is used to find the optimal number of hidden layers and nodes at each. According to the table, an ANN with two hidden layers and 50 nodes at each produces the greatest results, with accuracy rates of 99.6276% for training and 99.4023% for testing. This procedure requires about 46 seconds.

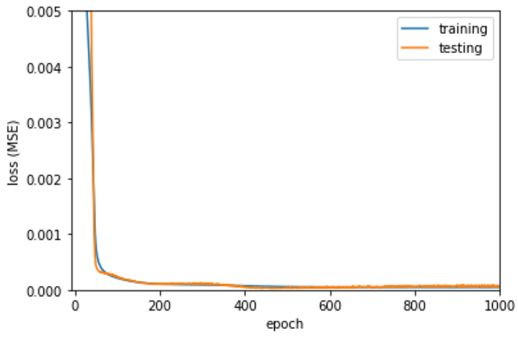

Figure 2. The convergence history of the loss function generated by combining Adam and ReLU for the FG plate

Following that, an initial XGBoost model with a maximum tree depth (max_depth) of 2 and a learning rate (eta) of 0.3 is investigated. First, the effect of the number of trees (n_estimators) on the

Table 2. The effect of the number of epoch on the accuracy of the training and testing processes in ANN

	epoch	100	500	1000	3000	5000
MSE	Training	4.17E-04	4.80E-05	1.37E-05	1.63E-05	5.81E-06
	Testing	3.90E-04	4.68E-05	3.60E-05	1.48E-05	1.60E-05
MAPE	Training	2.5200	0.6838	0.4550	0.3724	0.2398
	Testing	3.0516	1.1380	0.9773	0.5977	0.6001
Time (second)		2.0874	7.7083	16.1840	46.1856	83.6125

Table 3. The effect of the number of hidden layers and nodes at each on the accuracy of the training and testing processes in ANN

		1-hidden layer			2-hidden layer			3-hidden layer		
Number of nodes		10	50	100	10	50	100	10	50	100
MSE	Training	5.16E-04	5.05E-05	3.56E-05	5.15E-04	**1.63E-05**	7.67E-06	5.19E-04	5.48E-06	4.44E-06
	Testing	1.01E-03	3.41E-04	1.51E-04	9.37E-04	**1.48E-05**	3.12E-05	8.51E-04	2.01E-05	2.42E-05
MAPE	Training	3.0998	0.6932	0.5666	3.1128	**0.3724**	0.2881	3.1517	0.2734	0.2123
	Testing	5.9001	2.8518	1.9775	5.6237	**0.5977**	0.8206	5.2975	0.6978	0.7470
Time (second)		34.5629	39.4934	48.0315	36.4842	**46.1856**	59.3647	36.2287	49.7412	76.2092

Table 4. The effect of the number of trees on the accuracy of the training and testing processes in XGBoost

	n_estimators	10	30	50	100	150	200	500	1000
MSE	Training	1.67E-05	2.66E-06	1.61E-06	7.33E-07	4.61E-07	**3.72E-07**	3.44E-07	3.44E-07
	Testing	1.69E-05	3.26E-06	2.11E-06	1.10E-06	7.79E-07	**6.67E-07**	6.27E-07	6.27E-07
MAPE	Training	0.5197	0.2001	0.1513	0.0984	0.0761	**0.0684**	0.0659	0.0659
	Testing	0.5303	0.2213	0.1725	0.1184	0.0965	**0.0889**	0.0865	0.0865
Time (second)		0.7166	2.0292	3.2557	6.4880	9.4724	**11.8802**	23.2319	47.5805

Table 5. The effect of maximum depth of a tree on the accuracy of the training and testing processes in XGBoost

	max_depth	1	2	3	5	7	10
MSE	Training	5.75E-06	3.72E-07	3.85E-07	**2.88E-07**	2.24E-07	2.00E-07
	Testing	6.49E-06	6.67E-07	7.14E-07	**5.81E-07**	5.08E-07	4.77E-07
MAPE	Training	0.2711	0.0684	0.0729	**0.0584**	0.0489	0.0448
	Testing	0.2945	0.0889	0.0938	**0.0794**	0.0709	0.0670
Time (second)		7.7124	11.8802	11.1105	**11.1861**	12.0319	12.7157

accuracy of the training and testing processes will be explored. The obtained results including MSE, MAPE, and computational time are shown in Table 4. From the table, it can be seen that XGBoost with n_estimators of 200, 500, and 1000 give the best results; however, XGBoost with n_estimators of 200 takes just 11.8802 seconds, while those of 500 and 1000 take 23.2319 and 47.5805 seconds, respectively. Therefore, XGBoost with the number of trees of 200 is utilized to investigate the max_depth, and eta parameters on the accuracy of XGBoost for predicting dynamic behaviors of the FG plate. Table 5 shows the influence of the max_depth on the accuracy of the present method. The table shows that a max_depth of 5 is sufficient to guarantee the precision of the training and testing processes. Finally, XGBoost with n_estimators of 200 and max_depth of 5 is utilized to find an optimal learning

rate (eta) for XGBoost in this study. Table 6 shows that, in comparison to other values of eta, 0.1 provides the best accuracy (99.9706% for training and 99.9474% for testing).

Table 6. The effect of learning rate on the accuracy of the training and testing processes in XGBoost

	eta	0.1	0.2	0.3	0.5	0.7	1
MSE	Training	**8.89E-08**	2.13E-07	2.88E-07	3.06E-07	2.87E-07	2.57E-07
	Testing	**2.57E-07**	4.46E-07	5.81E-07	5.85E-07	5.69E-07	5.44E-07
MAPE	Training	**0.0294**	0.0486	0.0584	0.0633	0.0627	0.0617
	Testing	**0.0526**	0.0701	0.0794	0.0824	0.0828	0.0838
Time (second)		**15.6894**	11.8815	11.1861	10.2114	10.0426	9.7932

As can be seen from the investigations above, XGBoost with n_estimators of 200, max_depth of 5, and eta of 0.1 is the optimal model for predicting dynamic behavior of the FG plate. Deflection center versus time of the FG plate under sudden load predicted with input n_z of 10 by the optimal XGBoost model is presented in Fig. 3. From the figure, it can be seen that results obtained by the XGBoost agree well with the exact ones. In comparison to the optimal ANN model, the optimal XGBoost model performs better for this problem. With regard to accuracy, XGBoost reaches 99.9706% for training and 99.9474% for testing, while ANN achieves 99.6276% for training and 99.4023% for testing. Additionally, while ANN needs 46.1856 seconds for training and testing, XGBoost just needs 15.6894 seconds.

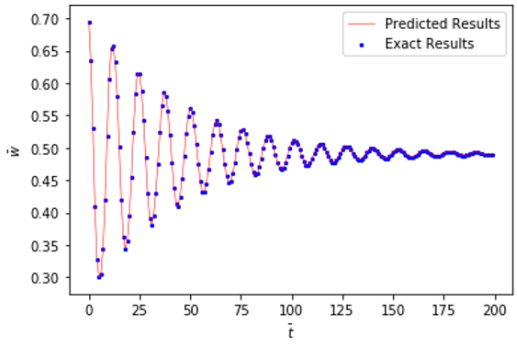

Figure 3. XGBoost model for predicting dynamic behavior of the FG plate

5. Conclusions

In this paper, ANN and XGBoost have been successfully developed for transient analysis of functionally graded plates with variations in material properties along the thickness direction. This study has examined a data set with one input, the power index, and 200 output values representing deflection versus time. Based on the data set, optimal weights for ANN and XGBoost have been found to predict the behavior of the plate without using any analysis tool. Moreover, the effect of parameters on the accuracy and computational time of two models have been investigated to find optimal models. The results of these optimal models and IGA have been compared. Based on the results, it is clear that XGBoost is not only superior to ANN in terms of accuracy and computational time, but it also ensures accuracy when compared to IGA. The current method can be applied to more complex engineering problems such as multi-directional functionally graded plates or shells. Moreover, optimization also awaits further attention.

Acknowledgements

This research is funded by Nguyen Tat Thanh University, Ho Chi Minh city, Vietnam.

References

[1] Klecka, J., Cizek, J., Matejicek, J., Lukac, F., Vala, J. (2023). Thick functionally-graded W-316L composite coatings for nuclear fusion applications. *Nuclear Materials and Energy*, 34:101373.

[2] Li, W., Han, B. (2018). Research and Application of Functionally Gradient Materials. *IOP Conference Series: Materials Science and Engineering*, 394:022065.

[3] Praveen, G. N., Reddy, J. N. (1998). Nonlinear transient thermoelastic analysis of functionally graded ceramic-metal plates. *International Journal of Solids and Structures*, 35(33):4457–4476.

[4] Ootao, Y., Ishihara, M. (2013). Three-dimensional solution for transient thermoelastic problem of a functionally graded rectangular plate with piecewise exponential law. *Composite Structures*, 106:672–680.

[5] Tran, M. T., Thai, S. (2023). Transient analysis of variable thickness multi-directional functionally graded plates using isogeometric analysis. *Multidiscipline Modeling in Materials and Structures*, 19(4):652–679.

[6] Zhang, X.-Y., Li, X.-F. (2019). Transient response of a functionally graded thermoelastic plate with a crack via fractional heat conduction. *Theoretical and Applied Fracture Mechanics*, 104:102318.

[7] Karakoti, A., Pandey, S., Kar, V. R. (2021). Nonlinear transient analysis of porous functionally graded material plates under blast loading. *Materials Today: Proceedings*, 46:8111–8113.

[8] Chen, T., Guestrin, C. (2016). XGBoost: A Scalable Tree Boosting System. In *Proceedings of the 22nd ACM SIGKDD International Conference on Knowledge Discovery and Data Mining*, KDD '16, ACM.

[9] Zhang, S., Shi, Z., Wang, G., Yan, R., Zhang, Z. (2022). Application of the extreme gradient boosting method to quantitatively analyze the mechanism of radon anomalous change in Banglazhang hot spring before the Lijiang Mw 7.0 earthquake. *Journal of Hydrology*, 612:128249.

[10] Zou, Y., Shi, Y., Sun, F., Liu, J., Guo, Y., Zhang, H., Lu, X., Gong, Y., Xia, S. (2022). Extreme gradient boosting model to assess risk of central cervical lymph node metastasis in patients with papillary thyroid carcinoma: Individual prediction using SHapley Additive exPlanations. *Computer Methods and Programs in Biomedicine*, 225:107038.

[11] Van Nguyen, D., Kim, D., Choo, Y. (2022). Optimized extreme gradient boosting machine learning for estimating diaphragm wall deflection of 3D deep braced excavation in sand. *Structures*, 45:1936–1948.

[12] Pant, A., Ramana, G. V. (2022). Prediction of pullout interaction coefficient of geogrids by extreme gradient boosting model. *Geotextiles and Geomembranes*, 50(6):1188–1198.

[13] Linh Khanh, P. N., Bao Ngan, N. H. (2023). Machine learning-based pedo transfer function for estimating the soil compression index. *Journal of Science and Technology in Civil Engineering (STCE) - HUCE*, 17 (1):67–78.

[14] Qui, L. X. (2023). Damage identification of trusses using limited modal features and ensemble learning. *Journal of Science and Technology in Civil Engineering (STCE) - HUCE*, 17(2):9–20.

[15] Hughes, T. J. R., Cottrell, J. A., Bazilevs, Y. (2005). Isogeometric analysis: CAD, finite elements, NURBS, exact geometry and mesh refinement. *Computer Methods in Applied Mechanics and Engineering*, 194(39–41):4135–4195.

[16] Son, T., Qui, L. X. (2022). Investigate the bending and free vibration responses of multi-directional functionally graded plates with variable thickness based on isogeometric analysis. *Journal of Science and Technology in Civil Engineering (STCE)-HUCE*, 16(4):10–29.

[17] Farahat, A., Verhelst, H. M., Kiendl, J., Kapl, M. (2023). Isogeometric analysis for multi-patch structured Kirchhoff–Love shells. *Computer Methods in Applied Mechanics and Engineering*, 411:116060.

[18] Yu, J., Yue, B., Ma, B. (2022). Isogeometric analysis with level set method for large-amplitude liquid sloshing. *Ocean Engineering*, 265:112613.

[19] Reddy, J. N. (1984). A Simple Higher-Order Theory for Laminated Composite Plates. *Journal of Applied Mechanics*, 51(4):745–752.

[20] Newmark, N. M. (1959). A Method of Computation for Structural Dynamics. *Journal of the Engineering Mechanics Division*, 85(3):67–94.

[21] Kant, T., Varaiya, J. H., Arora, C. P. (1990). Finite element transient analysis of composite and sandwich plates based on a refined theory and implicit time integration schemes. *Computers & Structures*, 36(3): 401–420.

[22] Lei, Z. X., Zhang, L. W., Liew, K. M. (2015). Elastodynamic analysis of carbon nanotube-reinforced functionally graded plates. *International Journal of Mechanical Sciences*, 99:208–217.